frontiers in Materials

ORIGINAL RESEARCH
published: 09 September 2021
doi: 10.3389/fmats.2021.727617

Halide Electrolyte Li_3InCl_6-Based All-Solid-State Lithium Batteries With Slurry-Coated $LiNi_{0.8}Co_{0.1}Mn_{0.1}O_2$ Composite Cathode: Effect of Binders

Kai Wang, Qing Ye, Jun Zhang, Hui Huang, Yongping Gan, Xinping He and Wenkui Zhang**

College of Materials Science and Engineering, Zhejiang University of Technology, Hangzhou, China

All-solid-state lithium batteries (ASSLBs) with solid-state electrolytes (SSEs) are considered as a promising next-generation energy storage technology due to their improved safety and higher energy density. Among various SSEs, halide Li_3InCl_6 is emerging as a promising candidate because of its high ionic conductivity, air-stability, and wide electrochemical window. Generally, most of the ASSLBs based on inorganic SSEs are assembled by mixed dry pressing, which is not easy, to achieve uniform dispersion of powder composite cathode. Here, a slurry coating method by dispersing active materials ($LiNi_{0.8}Co_{0.1}Mn_{0.1}O_2$), SSEs ($Li_3InCl_6$), binders (ethyl cellulose, polymethyl methacrylate, styrene butadiene rubber, and nitrile rubber), and conductive carbon black in toluene solvent is used to fabricate cathodes. We studied the effects of different kinds of binders and their contents on the electrochemical performance of ASSLBs. The results show that polymethyl methacrylate, ethyl cellulose, styrene butadiene rubber, and nitrile rubber binders are all suitable for preparing cathodes, and a binder content of 2 wt% can achieve the best electrochemical performance of the ASSLBs. This work proves that the intimate contact between the active material and the halide SSE in the electrode can be realized by using slurry coating method with suitable binders, thus achieving stable electrochemical performance.

Keywords: Li_3InCl_6, all-solid-state lithium batteries, solid electrolytes, binders, slurry coating

OPEN ACCESS

Edited by:
Yutao Li,
University of Texas at Austin, United States

Reviewed by:
Biyi Xu,
University of Texas at Austin, United States
Nan Wu,
Beijing Institute of Technology, China

****Correspondence:***
Jun Zhang
zhangjun@zjut.edu.cn
Wenkui Zhang
msechem@zjut.edu.cn

Specialty section:
This article was submitted to Energy Materials, a section of the journal Frontiers in Materials

Received: *19 June 2021*
Accepted: *05 July 2021*
Published: *09 September 2021*

Citation:
Wang K, Ye Q, Zhang J, Huang H, Gan Y, He X and Zhang W (2021) Halide Electrolyte Li_3InCl_6-Based All-Solid-State Lithium Batteries With Slurry-Coated $LiNi_{0.8}Co_{0.1}Mn_{0.1}O_2$ Composite Cathode: Effect of Binders. Front. Mater. 8:727617. doi: 10.3389/fmats.2021.727617

INTRODUCTION

Compared with traditional liquid lithium-ion batteries, all solid-state lithium batteries (ASSLBs) have better development prospects due to their improved safety, high-energy density, and thermal stability (Yue et al., 2017; Kraft et al., 2018; Zhang et al., 2018b). Solid-state electrolytes (SSEs) are the key material of the next-generation ASSLBs (Kamaya et al., 2011; Janek and Zeier 2016; Zhang et al., 2018b). Inorganic solid electrolyte has become a research hotspot in the field of electrolyte because of its advantages of stable chemical and electrochemical properties and high ionic conductivity at room temperature (Kamaya et al., 2011; Nam et al., 2015; Kato et al., 2016). Compared with the traditional organic electrolyte, the electrochemical window of the SSEs is as high as 5 V or more and can be equipped with high-voltage positive electrode materials (Feinauer et al., 2019), thus effectively improving the energy density and safety of the battery (Wang et al., 2019b). In addition, the SSEs can play the dual roles of separator and electrolyte, which can simplify the internal structure and

packaging process of the battery and reduce the manufacturing cost (Quartarone and Mustarelli 2011; Chen et al., 2016).

In the past few years, great progress has been made in the research of SSEs (Bachman et al., 2016). At present, the research on inorganic SSEs mainly focuses on sulfide-based SSEs (Seino et al., 2014) and oxide SSEs(Liu et al., 2018; Wang et al., 2019a). Among them, sulfide-based SSEs usually exhibit high ionic conductivity (10^{-3} ~ 10^{-4} S/cm) at room temperature (Seino et al., 2014; Kato et al., 2016). Second, sulfide SSEs also have good thermal stability, wide electrochemical window, and excellent mechanical properties (Adeli et al., 2019). However, sulfide SSEs are extremely unstable in the atmosphere and easily reacts with water and oxygen to generate highly toxic H_2S gas (Xu et al., 2018). Moreover, the direct contact between sulfide SSEs and positive electrode component leads to large interfacial resistance due to inevitable side reactions, and this situation will be aggravated by decomposition of sulfide SSEs at high voltage (Deiseroth et al., 2008; Boulineau et al., 2012). Compared with sulfide SSEs, oxide SSEs have excellent air stability. However, the interface between the oxide SSEs and the electrode will produce a large interface impedance. Moreover, the synthesis process of oxide SSEs requires high-temperature sintering, which will lead to side reactions between electrode and oxide SSEs during co-sintering (Deng et al., 2015). These unfavorable factors hinder the further development of oxide SSEs (Thangadurai et al., 2014; Uhlmann et al., 2016). Therefore, it is still challenging to find SSEs materials with high ionic conductivity, electrochemical stability, chemical stability, and deformability (Bachman et al., 2016). Recently, great progress has been made in the research of halide SSEs (Li et al., 2020). Most of the obstacles of oxides and sulfides mentioned above are no longer the problem of halide SSEs (Li et al., 2019b). It has been reported that the ionic conductivity of Li_3MX_6 (M is a metal element, and X is a halogen) SSEs can reach 10^{-3} S/cm at room temperature (Asano et al., 2018; Li et al., 2019b; Park et al., 2020). Moreover, the halide solid electrolyte has a wide electrochemical window exceeding 4V (Liang et al., 2020). In halide SSEs systems, it has been proved that Li_3InCl_6 SSE is stable under dry oxygen atmosphere, and its water absorption and dehydration process are reversible under atmospheric atmosphere (Li et al., 2019b).

At present, ASSLBs based on Li-M-X system SSEs usually use mixed dry pressing method to prepare a positive electrode. The positive electrode prepared by mixed dry pressing has poor contact between electrode material and SSEs, which will produce large charge transfer resistance and affect the electrochemical performance of the battery (Zhou et al., 2016). In addition, the preparation of positive electrode of lithium battery by mixed dry pressing is not easy to achieve uniform dispersion of powder composite cathode and is not conducive to commercial large-scale production (Jung et al., 2015). Simultaneously, during the cycle of the battery, the process of lithium ion lithiation/delithiation will generate a tremendous strain/stress, which will cause separation between active materials and SSEs and affect the performance of the ASSLBs (Liang et al., 2016). On the contrary, the cathodes prepared by the slurry coating method can be closely contacted with the active materials under the action of binder, and dispersed evenly with each other, which can effectively reduce the interfacial resistance (Banerjee et al., 2016). This is because the rich functional groups of polymer binder can make the components in the cathodes well-combined through chemical bond adsorption (Park et al., 2016). Moreover, the long chain structure of polymer binder will also provide mechanical resistance to the volume change of electrode during battery cycle, thus alleviating this problem (Nam et al., 2018). Therefore, finding a suitable binder is very important to realize the long cycle of ASSLBs.

In this work, we select suitable binders for preparing the positive electrodes of ASSLBs using the slurry coating method. In the cathodes, Li_3InCl_6 is used as SSEs, $Ni_{0.8}Co_{0.1}Mn_{0.1}O_2$ (NCM) is used as active materials, and carbon black is used as conductive additive. The ASSLBs is assembled with Li_3InCl_6 solid electrolyte and prepared positive electrode. We studied the influence of various binder type and contents on the electrochemical performance of ASSLBs. The results show that different binder contents have a great influence on the electrochemical performance of ASSLBs. Thus, a proper binder content plays a vital role in improving the performance of ASSLBs.

EXPERIMENTAL

Material Synthesis

Synthesis of Li_3InCl_6: lithium chloride (LiCl, Alfa Aesar, 99.9%) and indium chloride ($InCl_3$, Alfa Aesar, 99.99%) were weighed to the stoichiometric molar ratio. The mixtures were mechanically mixed in a ZrO_2 pot with ZrO_2 balls. The mixing process was performed using a planetary ball milling apparatus at 500 rpm for 24 h. All the preparation processes were carried out with an Ar atmosphere. Several hundreds of milligrams of the ball-milled Li_3InCl_6 were pelletized at 200 MPa, sealed in a glass tube under vacuum, annealed at 260–400°C for different duration (2–12 h), and cooled to room temperature in 2 h.

Preparation of cathode composite: the target ratio of binders is dissolved in an appropriate amount of toluene solution. $LiNi_{0.8}Co_{0.1}Mn_{0.1}O_2$, Li_3InCl_6 solid electrolyte and carbon black are added to the above solution and stirred to prepare a slurry. Then the slurry is evenly coated on the aluminum foil and dried. The mass loading of the active material in the electrode is about 0.8 mg.

Material Characterizations

The crystal phase and structure of the synthesized sample were characterized by Rigaku Ultima IV X-ray diffraction (XRD). The morphology, microstructure, and chemical composition of the prepared electrode were characterized by a scanning electron microscope (SEM, Hitachi S4700) equipped with energy dispersive spectroscopy (EDS). The impedance of the prepared Li_3InCl_6 SSE was measured with a ZENNIUM electrochemical workstation in the frequency range of 4 MHz–10 Hz with a voltage amplitude of 10 mV.

Electrochemical Measurements

The ASSLBs were fabricated using the prepared annealed-Li_3InCl_6 SSEs inside the Ar-filled glovebox. The slurry coating

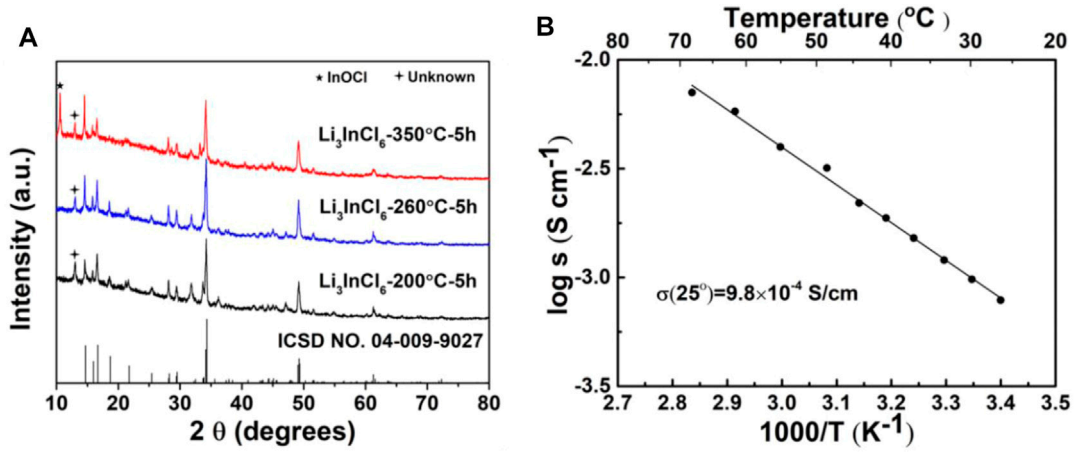

FIGURE 1 | (A) XRD patterns of annealed Li_3InCl_6 sample. **(B)** Temperature dependence of the ionic conductivity for Li_3InCl_6 solid electrolyte.

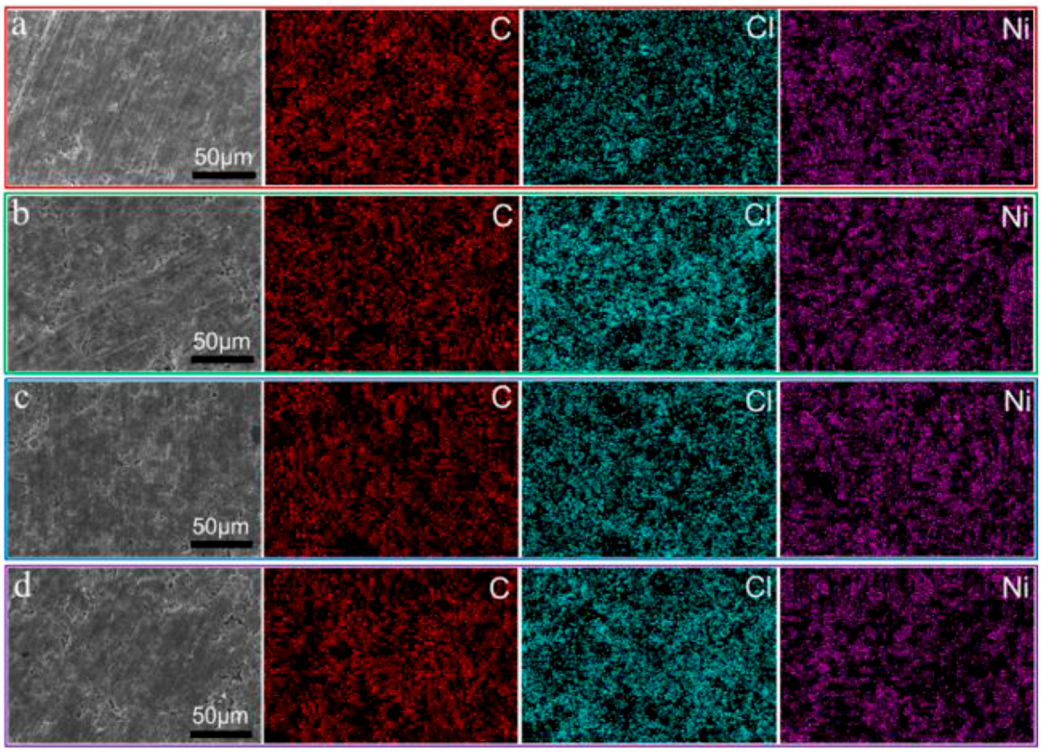

FIGURE 2 | SEM images of electrode with 2wt% binders and the corresponding element mapping **(A)** PMMA, **(B)** EC, **(C)** SBR, and **(D)** NBR.

method is used to prepare the positive electrode. Various components were dispersed in toluene containing 15% Li_3InCl_6, 75% the NCM, binder, and carbon black. We selected four binder materials, namely polymethyl methacrylate (PMMA), ethyl cellulose (EC), styrene-butadiene rubber (SBR), and nitrile rubber (NBR). These four binders can be well-dissolved in the toluene solution to form a uniform slurry. At the same time, taking the content of each binder as a variable, the influence of each binder on the ASSLBs performance was studied. Uniform slurry is coated on charcoal-coated aluminum foil, and then naturally dried. The dried positive electrode was laid flat on the bottom of a stainless steel mold with a diameter of 12 mm. Then, 70 mg of annealed Li_3InCl_6 SSE powder was evenly spread on the positive electrode and pressed into a wafer under a

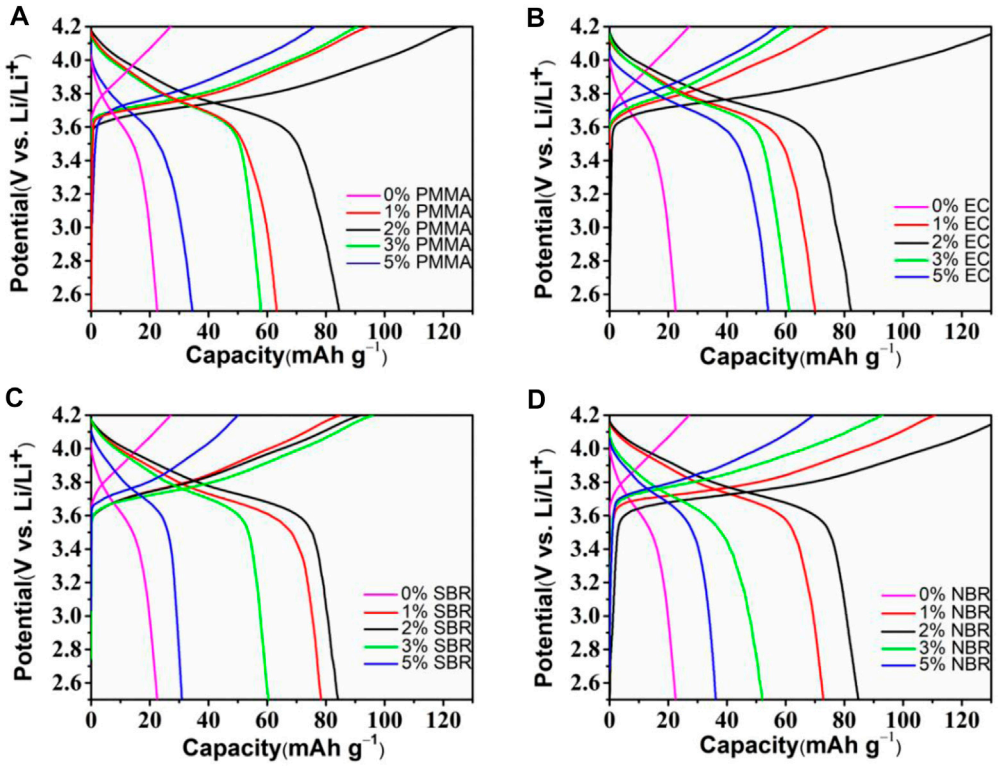

FIGURE 3 | Initial charge–discharge profiles of cathode composites with different amount of binder **(A)** PMMA, **(B)** EC, **(C)** SBR, and **(D)** NBR.

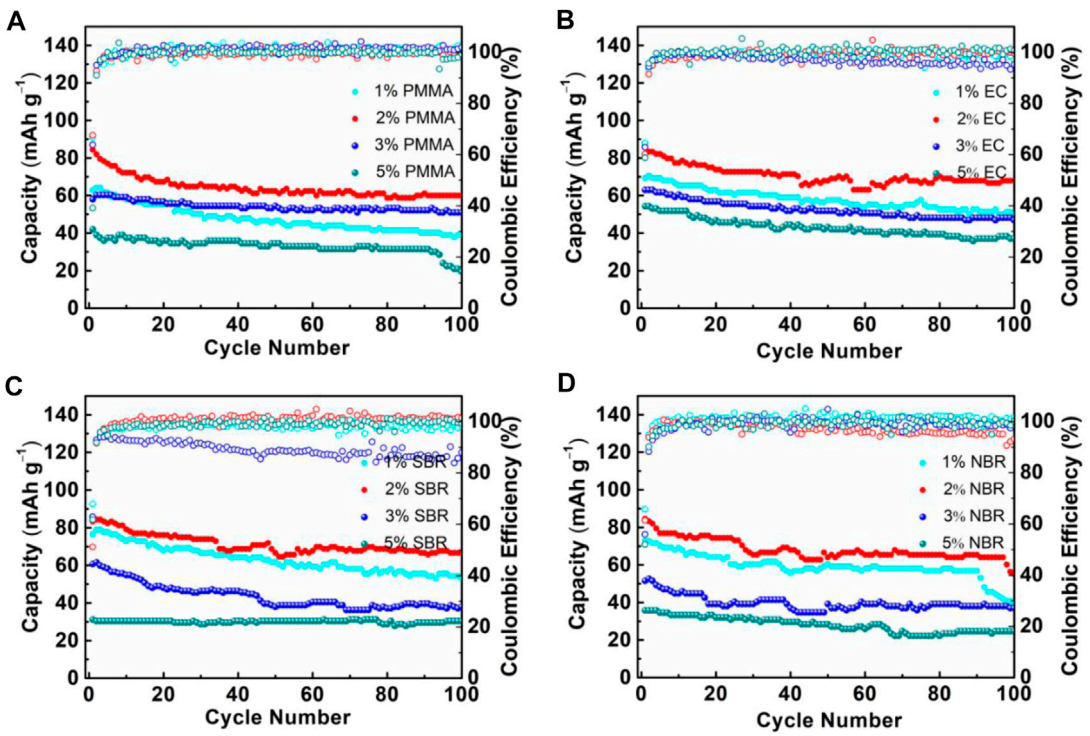

FIGURE 4 | Cycling performance at 0.05C of cathode composites with different amount of binder **(A)** PMMA, **(B)** EC, **(C)** SBR, and **(D)** NBR.

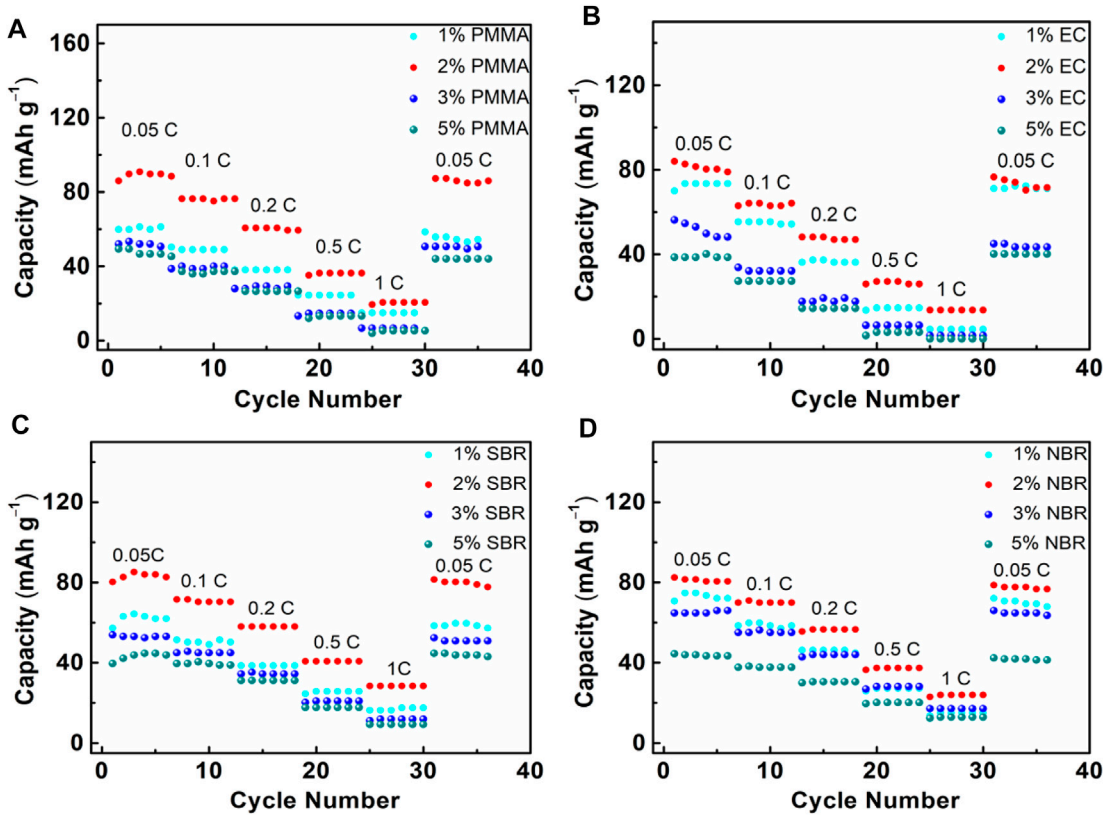

FIGURE 5 | Rate performance of cathode composites with different amount of binder **(A)** PMMA, **(B)** EC, **(C)** SBR, and **(D)** NBR.

pressure of 30 Mpa. Another 30 mg of Li_6PS_5Cl (Yu et al., 2016) was further added to avoid the possible influence of redox conversion between In^{3+} and Li foil anode. A 0.8 mm thick lithium metal foil (Oujin, Shanghai, China) is pressed on the other side of the SSE layer as a counter electrode. The galvanostatic charge–discharge studies of NCM cathodes were conducted at different current densities (e.g., 1C = 200 mA g^{-1}), within a potential window of 2.5–4.2 V vs. Li/Li^+ at 25°C.

RESULT AND DISCUSSION

Figure 1A shows a typical X-ray diffraction (XRD) pattern of annealed Li_3InCl_6 sample. It could be found that a peak corresponding to InOCl is observed in the XRD pattern of the Li_3InCl_6 sample annealed at 350°C. This indicates that the impure phase InOCl appears in the Li3InCl6 sample during annealing. An unknown weak peak appears in the XRD pattern of the sample annealed at 200°C. When the annealing temperature is increased to 260°C, the intensity of the unknown peak weakens. The ionic conductivity of the Li3InCl6 SSE obtained at 260°C was studied by electrochemical impedance spectroscopy. The temperature dependence of the ionic conductivity of the Li_3InCl_6 SSE is shown in **Figure 1B**. The plotted ionic conductivities were calculated from the sum of the grain boundary and bulk resistance featured with a semicircle in the high frequency region (Zhang et al., 2018a). At room temperature, Li_3InCl_6 solid electrolyte exhibits an ionic conductivity of 9.8×10^{-4} S cm^{-1}, which is slightly lower than previously reported (Huang et al., 2019; Li et al., 2019a). This is due to a small amount of impurity phase in annealed Li_3InCl_6.

To study the morphologies and elemental distribution of various components in the cathodes, EDS and scanning electron microscopy (SEM) are further performed. **Figure 2** shows the SEM image of electrode and the corresponding element mappings. **Figures 2A–D** are SEM and EDS of the cathodes prepared with PMMA, EC, SBR, and NBR as binders, respectively. The results show that after compaction, the surface of the positive electrode is flat and there are no large cracks and potholes. It shows that the Li_3InCl_6 SSEs, NCM particles, and carbon black in the positive electrode are in close contact with each other due to the adhesion of binder. Under the influence of the long chain structure of binder and the adsorption of functional groups, the components in the cathode are tightly combined. Moreover, the electrode is closely attached to the carbon coated aluminum foil current collector (**Supplementary Figure S3**), which will increase the electronic conductivity, indicating the importance of the adhesion of the

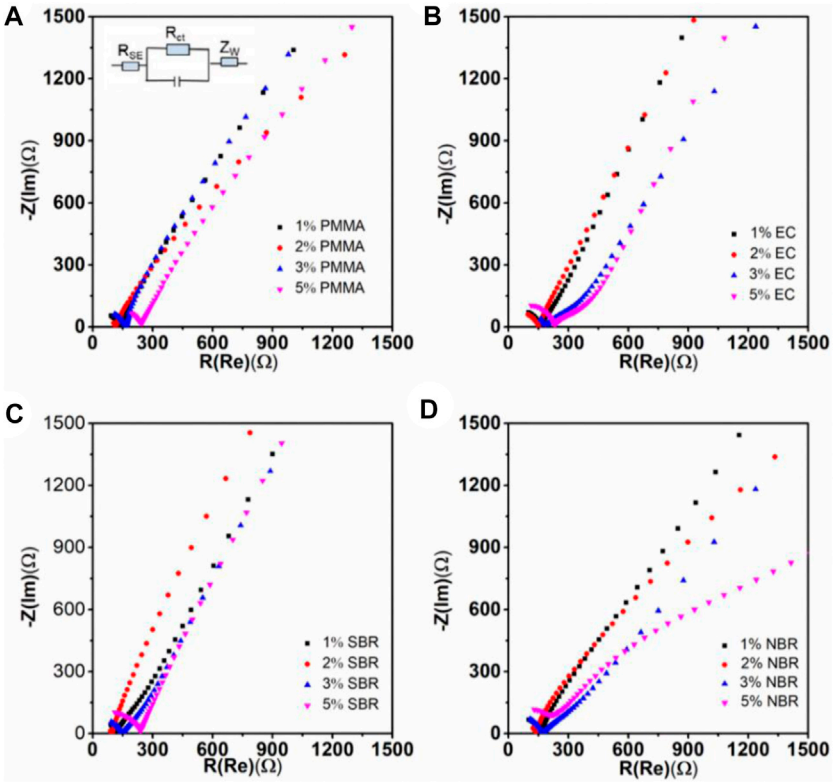

FIGURE 6 | Nyquist plots of cathode composites with various amount of binders: **(A)** PMMA, **(B)** EC, **(C)** SBR, and **(D)** NBR.

binder. On the other hand, it can be found from EDS mapping that nickel, carbon, and chlorine are evenly distributed on the electrode. This suggests that during the slurry coating process, Li_3InCl_6 SSEs, active material particles, and carbon black in the positive electrode are evenly dispersed due to the adhesion of binder dissolved in toluene solution. This plays a vital role in the electrochemical performance of ASSLBs. As shown in **Supplementary Figure S2**, this finding can also be confirmed from the cross-sectional SEM image of the electrode and the corresponding element mappings. Meanwhile, it can be found that Li_3InCl_6 SSE is filled between NCM particles, which are conducive to the conduction of lithium ions at the interface. The NCM particles are tightly coated with the Li_3InCl_6 SSE, which further confirms that the NCM particles are in close contact with the Li_3InCl_6 SSE under the influence of the binder. This is conducive to the fast Li^+ transportation and improves the electrochemical performance of the ASSLBs.

To investigate the electrochemical behaviors of the positive electrode with binder, we assembled ASSLBs with the electrode containing different binders. **Figure 3A** displays the initial discharge/charge capacity of composite electrodes with different contents of PMMA binder at a current density of 0.05 C. For the ASSLBs without any binder, the discharge capacity of the first cycle is only 22 mA h g^{-1}, and the corresponding coulombic efficiency is 28.5%. Because there is no binder in the electrode, the contact between Li_3InCl_6 SSE and active materials is poor, which leads to the difficulty of lithium ions conduction in the electrode area and affects lithiation/delithiation of lithium ions during charging and discharging. Compared with the battery without binder, the discharge capacity of the battery with PMMA binder is improved. It can be found that the electrode containing 2 wt% PMMA binder delivers the highest discharge capacity. And when the content of binder in the electrode increases or decreases, the discharge capacity of ASSLBs will decrease. This is because when the binder without lithium ions conductivity in the electrode increases, the charge transfer resistance at the electrode interface increases, the lithium ions conductivity decreases, and the lithium ions diffusion channel decreases. However, when the binder in the electrode is further reduced, the limited binder is not enough to provide sufficient adhesion for the formation of close contact between Li_3InCl_6 SSE and NCM active material, resulting in the contact between the two is not close enough, and the diffusion channel of lithium ions will also be reduced. At the same time, the initial coulombic efficiency of the electrode with 2 wt% binder can reach 67.5%, which shows that the appropriate binder content can effectively increase the initial reversible capacity. Therefore, 2 wt % PMMA binder is the most suitable percentage for the electrode. **Figures 3B–D** corresponds to the initial discharge/

charge curves of electrodes with EC, SBR, and NBR binders at a current density of 0.05 C, respectively. It can be found that for EC, SBR, and NBR binders, when the binder content in the composite electrode is 2 wt%, the capacity of ASSLBs is the highest. It can be seen that, for Li_3InCl_6 SSE, when the coating method is used to prepare the electrode and PMMA, EC, SBR, and NBR are used as binders, the binder content of 2 wt% is suitable. At the same time, when the binder content is controlled at 2 wt%, the interface formed by Li_3InCl_6 SSE and active materials can provide more lithium ions migration channels, which is beneficial to lithium ions conduction. To study the electrochemical behaviors, we examined the cyclic voltammetry (CV) of NCM cathodes with EC, SBR, and NBR binder. As shown in **Supplementary Figure S4**, the CV curves were tested at a constant sweep rate of 0.1 mV s^{-1} in the voltage range of 2.5–4.2 V. One oxidation peak and one reduction peak can be observed, corresponding to the insertion and extraction of lithium ions, respectively.

In order to evaluate battery performance using electrodes with different binder, ASSLBs were fabricated. **Figure 4** shows the long-term cycling performance of batteries with different binders and different contents at 0.05C and 30°C. The long-term cycling performance for the batteries with PMMA binder using different content binder is shown in **Figure 4A**. For the ASSLB with PMMA binder, ASSLBs with 2 wt% binder maintains a reversible capacity of 84 mA h g^{-1} with a capacity retention of 71.4% after 100 cycles. At the same time, the battery with 1 wt%, 3 wt%, and 5 wt% PMMA binder maintains a reversible capacity of 39 mA h g^{-1}, 51 mAh g^{-1}, and 30 mAh g^{-1}, respectively. **Figure 4B** compares the long cycling performance for the batteries with EC binder using different content binder. Obviously, the cycling stability and reversible capacity of ASSLBs with 2 wt% EC binder are more excellent than those of the ASSLBs with other binder content, with a specific capacity of 70 mAh g^{-1} remaining after 100 cycles. **Figure 4C** displays the long-term cycling performance for the batteries with SBR binder and different contents. The reason for this situation is mainly due to insufficient binder in the composite electrode, which leads to insufficient contact between the SSEs and the active materials. During the battery cycle, lithiation/delithiation of lithium ions will make this phenomenon more serious. On the other hand, the battery with 3 wt% binder and 4 wt% binder in the electrodes exhibits lower capacity, which is due to the excess binder covering the active material. **Figure 4D** shows the long-term cycling performance of the positive electrodes with different NBR binder content. The electrode with 2 wt% NBR binder showed the highest discharge capacity and the smallest capacity reduction after 100 cycles. Compared with previous related reports (Zhang et al., 2018a), the discharge capacity of this work is slightly lower.

To further discuss the influence of different binder content on the rate performance of the electrode, the ASSLBs were tested under different current densities from 0.05 to 1 C at room temperature. **Figure 5** displays the rate capability of the ASSLBs which use NCM composite electrode with PMMA, EC, SBR, and NBR binder. As shown in **Figure 5A**, the ASSLBs with PMMA binder showed an acceptable rate capability. Upon discharging at current densities of 0.05, 0.1, 0.2, 0.5, and 1 C, reversible capacities of 87, 76, 60, 35, and 20 mA h g^{-1} are achieved, respectively. On the other hand, the ASSLBs with EC, SBR, and NBR binder delivered acceptable rate performances as well. Therefore, PMMA, EC, SBR, and NBR binder are applicable binders for ASSLBs with the Li_3InCl_6 SSE when the cathode of the battery is prepared by slurry coating method. Since the reversible capacity was recovered when returning to a lower current density, it is speculated that there is no serious separation between the active materials and Li_3InCl_6 SSE. This is mainly due to the close contact between the NCM particles and the Li_3InCl_6 SSE under the action of the binder.

It is well-known that interface impedance is a critical factor for performances of ASSLBs(Bohnsack et al., 1997; Li et al., 2019a). To further understand the interface compatibility between the SSE and the electrode, electrochemical impedance spectroscopy (EIS) tests of the ASSLBs were performed to evaluate the resistance of the electrode prior to cycling. **Figure 6** displays the impedance profiles of the ASSLBs. The impedance values corresponding to the intersection of the high frequency semicircle and the low frequency semicircle with the horizontal axis are the SSE layer impedance R_{SE} and the interface charge transfer resistance R_{ct} between the electrode and the SSEs interface, respectively (Deng et al., 2015). Clearly, the cathode with 2 wt% binder shows the smallest resistance. Because the polymer binder does not have lithium ions conductivity, when the binder content in the electrode increases, the electrode interface impedance increases. However, when the content of binder in the electrode decreases, the interface impedance of the electrode also increases. This is because when the binder content in the electrode decreases, there is not enough binder to achieve close contact between the positive electrode active material NCM particles and the Li_3InCl_6 SSE, resulting in an increase in electrode interface impedance.

CONCLUSION

In summary, we successfully prepared positive electrodes with PMMA, EC, SBR, or NBR as binders, Li_3InCl_6 as solid electrolyte, carbon black as electron conduction agent, and $LiNi_{0.8}Co_{0.1}Mn_{0.1}O_2$ (NCM) as the active material. And the ASSLBs are assembled with a positive electrode prepared by a slurry coating method. The results show that the electrodes prepared by slurry coating method have low interfacial impedance due to the intimate contact between NCM particles and the SSE. In addition, content of binder has a great influence on the electrochemical performance of ASSLBs. The ASSLBs containing 2 wt% binder showed the better electrochemical performance, which indicated that 2 wt% binder content was the most suitable ratio. Our results suggest that PMMA, EC, SBR, and NBR can all be used in the preparation of positive electrodes for all-solid-state batteries, but a moderate content of binder has a crucial influence on the improvement of the electrochemical performance of all-solid-state batteries. Nevertheless, for practical use of Li_3InCl_6 solid electrolyte in slurry coating electrodes, further efforts are needed to improve the utilization rate of active material with higher mass loading.

DATA AVAILABILITY STATEMENT

The raw data supporting the conclusion of this article will be made available by the authors, without undue reservation.

AUTHOR CONTRIBUTIONS

KW: experiment, data curation, and writing—original draft. QY: characterizations. JZ: conceptualization, methodology, writing—review and editing. HH: methodology. YG and XH: data curation. WZ: supervision.

ACKNOWLEDGMENTS

The authors acknowledge the support by Zhejiang Provincial Natural Science Foundation of China (No. LR20E020002) and the National Natural Science Foundation of China (NSFC) under grant Nos U20A20253 and 21972127.

SUPPLEMENTARY MATERIAL

The Supplementary Material for this article can be found online at: https://www.frontiersin.org/articles/10.3389/fmats.2021.727617/full#supplementary-material

REFERENCES

Adeli, P., Bazak, J. D., Park, K. H., Kochetkov, I., Huq, A., Goward, G. R., et al. (2019). Boosting Solid-State Diffusivity and Conductivity in Lithium Superionic Argyrodites by Halide Substitution. *Angew. Chem. Int. Ed.* 58 (26), 8681–8686. doi:10.1002/anie.201814222

Asano, T., Sakai, A., Ouchi, S., Sakaida, M., Miyazaki, A., and Hasegawa, S. (2018). Solid Halide Electrolytes with High Lithium-Ion Conductivity for Application in 4 V Class Bulk-type All-Solid-State Batteries. *Adv. Mater.* 30 (44), 1803075. doi:10.1002/adma.201803075

Bachman, J. C., Muy, S., Grimaud, A., Chang, H.-H., Pour, N., Lux, S. F., et al. (2016). Inorganic Solid-State Electrolytes for Lithium Batteries: Mechanisms and Properties Governing Ion Conduction. *Chem. Rev.* 116 (1), 140–162. doi:10.1021/acs.chemrev.5b00563

Banerjee, A., Park, K. H., Heo, J. W., Nam, Y. J., Moon, C. K., Oh, S. M., et al. (2016). Na3 SbS4 : A Solution Processable Sodium Superionic Conductor for All-Solid-State Sodium-Ion Batteries. *Angew. Chem. Int. Ed.* 55 (33), 9634–9638. doi:10.1002/anie.201604158

Bohnsack, A., Balzer, G., Gudel, H.-U., Wickleder, M. S., and Meyer, G. (1997). Ternare Halogenide Vom Typ A3MX6. VII [1]. Die Bromide Li3MBr6 (M=Sm? Lu, Y): Synthese, Kristallstruktur, Ionenbeweglichkeit Lu, Y): Synthese, Kristallstruktur, Ionenbeweglichkeit. *Z. Anorg. Allg. Chem.* 623 (9), 1352–1356. doi:10.1002/zaac.19976230905

Boulineau, S., Courty, M., Tarascon, J.-M., and Viallet, V. (2012). Mechanochemical Synthesis of Li-Argyrodite Li6PS5X (X=Cl, Br, I) as Sulfur-Based Solid Electrolytes for All Solid State Batteries Application. *Solid State Ionics* 221, 1–5. doi:10.1016/j.ssi.2012.06.008

Chen, R., Qu, W., Guo, X., Li, L., and Wu, F. (2016). The Pursuit of Solid-State Electrolytes for Lithium Batteries: from Comprehensive Insight to Emerging Horizons. *Mater. Horiz.* 3 (6), 487–516. doi:10.1039/C6MH00218H

Deiseroth, H.-J., Kong, S.-T., Eckert, H., Vannahme, J., Reiner, C., Zaiß, T., et al. (2008). Li6PS5X: A Class of Crystalline Li-Rich Solids with an Unusually High Li+ Mobility. *Angew. Chem. Int. Ed.* 47 (4), 755–758. doi:10.1002/anie.200703900

Deng, Y., Eames, C., Chotard, J.-N., Lalère, F., Seznec, V., Emge, S., et al. (2015). Structural and Mechanistic Insights into Fast Lithium-Ion Conduction in Li4SiO4-Li3PO4 Solid Electrolytes. *J. Am. Chem. Soc.* 137 (28), 9136–9145. doi:10.1021/jacs.5b04444

Feinauer, M., Euchner, H., Fichtner, M., and Reddy, M. A. (2019). Unlocking the Potential of Fluoride-Based Solid Electrolytes for Solid-State Lithium Batteries. *ACS Appl. Energ. Mater.* 2 (10), 7196–7203. doi:10.1021/acsaem.9b01166

Huang, Y., Yang, C., Deng, B., Wang, C., Li, Q., De Villenoisy Thibault, C., et al. (2019). Nanostructured Pseudocapacitors with pH-Tunable Electrolyte for Electrochromic Smart Windows. *Nano Energy* 66, 104200. doi:10.1016/j.nanoen.2019.104200

Janek, J., and Zeier, W. G. (2016). A Solid Future for Battery Development. *Nat. Energ.* 1 (9), 16141. doi:10.1038/nenergy.2016.141

Jung, Y. S., Oh, D. Y., Nam, Y. J., and Park, K. H. (2015). Issues and Challenges for Bulk-type All-Solid-State Rechargeable Lithium Batteries Using Sulfide Solid Electrolytes. *Isr. J. Chem.* 55 (5), 472–485. doi:10.1002/ijch.201400112

Kamaya, N., Homma, K., Yamakawa, Y., Hirayama, M., Kanno, R., Yonemura, M., et al. (2011). A Lithium Superionic Conductor. *Nat. Mater* 10 (9), 682–686. doi:10.1038/nmat3066

Kato, Y., Hori, S., Saito, T., Suzuki, K., Hirayama, M., Mitsui, A., et al. (2016). High-power All-Solid-State Batteries Using Sulfide Superionic Conductors. *Nat. Energ.* 1 (4), 16030. doi:10.1038/nenergy.2016.30

Kraft, M. A., Ohno, S., Zinkevich, T., Koerver, R., Culver, S. P., Fuchs, T., et al. (2018). Inducing High Ionic Conductivity in the Lithium Superionic Argyrodites Li6+xP1-xGexS5I for All-Solid-State Batteries. *J. Am. Chem. Soc.* 140 (47), 16330–16339. doi:10.1021/jacs.8b10282

Li, X., Liang, J., Chen, N., Luo, J., Adair, K. R., Wang, C., et al. (2019a). Water-Mediated Synthesis of a Superionic Halide Solid Electrolyte. *Angew. Chem. Int. Ed.* 58 (46), 16427–16432. doi:10.1002/anie.201909805

Li, X., Liang, J., Luo, J., Norouzi Banis, M., Wang, C., Li, W., et al. (2019b). Air-stable Li3InCl6 Electrolyte with High Voltage Compatibility for All-Solid-State Batteries. *Energy Environ. Sci.* 12 (9), 2665–2671. doi:10.1039/C9EE02311A

Li, X., Liang, J., Yang, X., Adair, K. R., Wang, C., Zhao, F., et al. (2020). Progress and Perspectives on Halide Lithium Conductors for All-Solid-State Lithium Batteries. *Energ. Environ. Sci.* 13 (5), 1429–1461. doi:10.1039/C9EE03828K

Liang, J., Li, X., Wang, S., Adair, K. R., Li, W., Zhao, Y., et al. (2020). Site-Occupation-Tuned Superionic LixScCl3+xHalide Solid Electrolytes for All-Solid-State Batteries. *J. Am. Chem. Soc.* 142 (15), 7012–7022. doi:10.1021/jacs.0c00134

Liang, S., Liang, C., Xia, Y., Xu, H., Huang, H., Tao, X., et al. (2016). Facile Synthesis of Porous Li2S@C Composites as Cathode Materials for Lithium-Sulfur Batteries. *J. Power Sourc.* 306, 200–207. doi:10.1016/j.jpowsour.2015.12.030

Liu, Y., Sun, Q., Wang, D., Adair, K., Liang, J., and Sun, X. (2018). Development of the Cold Sintering Process and its Application in Solid-State Lithium Batteries. *J. Power Sourc.* 393, 193–203. doi:10.1016/j.jpowsour.2018.05.015

Nam, Y. J., Cho, S.-J., Oh, D. Y., Lim, J.-M., Kim, S. Y., Song, J. H., et al. (2015). Bendable and Thin Sulfide Solid Electrolyte Film: A New Electrolyte Opportunity for Free-Standing and Stackable High-Energy All-Solid-State Lithium-Ion Batteries. *Nano Lett.* 15 (5), 3317–3323. doi:10.1021/acs.nanolett.5b00538

Nam, Y. J., Oh, D. Y., Jung, S. H., and Jung, Y. S. (2018). Toward Practical All-Solid-State Lithium-Ion Batteries with High Energy Density and Safety: Comparative Study for Electrodes Fabricated by Dry- and Slurry-Mixing Processes. *J. Power Sourc.* 375, 93–101. doi:10.1016/j.jpowsour.2017.11.031

Park, K.-H., Kaup, K., Assoud, A., Zhang, Q., Wu, X., and Nazar, L. F. (2020). High-voltage Superionic Halide Solid Electrolytes for All-Solid-State Li-Ion Batteries. *ACS Energ. Lett.* 5 (2), 533–539. doi:10.1021/acsenergylett.9b02599

Park, K. H., Oh, D. Y., Choi, Y. E., Nam, Y. J., Han, L., Kim, J.-Y., et al. (2016). Solution-Processable Glass LiI-Li4 SnS4 Superionic Conductors for All-Solid-State Li-Ion Batteries. *Adv. Mater.* 28 (9), 1874–1883. doi:10.1002/adma.201505008

Quartarone, E., and Mustarelli, P. (2011). Electrolytes for Solid-State Lithium Rechargeable Batteries: Recent Advances and Perspectives. *Chem. Soc. Rev.* 40 (5), 2525–2540. doi:10.1039/C0CS00081G

Seino, Y., Ota, T., Takada, K., Hayashi, A., and Tatsumisago, M. (2014). A Sulphide Lithium Super Ion Conductor Is superior to Liquid Ion Conductors for Use in

Rechargeable Batteries. *Energ. Environ. Sci.* 7 (2), 627–631. doi:10.1039/C3EE41655K

Thangadurai, V., Narayanan, S., and Pinzaru, D. (2014). Garnet-type Solid-State Fast Li Ion Conductors for Li Batteries: Critical Review. *Chem. Soc. Rev.* 43 (13), 4714–4727. doi:10.1039/C4CS00020J

Uhlmann, C., Braun, P., Illig, J., Weber, A., and Ivers-Tiffée, E. (2016). Interface and Grain Boundary Resistance of a Lithium Lanthanum Titanate (Li3xLa2/3−xTiO3, LLTO) Solid Electrolyte. *J. Power Sourc.* 307, 578–586. doi:10.1016/j.jpowsour.2016.01.002

Wang, D., Sun, Q., Luo, J., Liang, J., Sun, Y., Li, R., et al. (2019a). Mitigating the Interfacial Degradation in Cathodes for High-Performance Oxide-Based Solid-State Lithium Batteries. *ACS Appl. Mater. Inter.* 11 (5), 4954–4961. doi:10.1021/acsami.8b17881

Wang, S., Bai, Q., Nolan, A. M., Liu, Y., Gong, S., Sun, Q., et al. (2019b). Lithium Chlorides and Bromides as Promising Solid-State Chemistries for Fast Ion Conductors with Good Electrochemical Stability. *Angew. Chem. Int. Ed.* 58 (24), 8039–8043. doi:10.1002/anie.201901938

Xu, R. C., Wang, X. L., Zhang, S. Z., Xia, Y., Xia, X. H., Wu, J. B., et al. (2018). Rational Coating of Li 7 P 3 S 11 Solid Electrolyte on MoS 2 Electrode for All-Solid-State Lithium Ion Batteries. *J. Power Sourc.* 374, 107–112. doi:10.1016/j.jpowsour.2017.10.093

Yu, C., van Eijck, L., Ganapathy, S., and Wagemaker, M. (2016). Synthesis, Structure and Electrochemical Performance of the Argyrodite Li 6 PS 5 Cl Solid Electrolyte for Li-Ion Solid State Batteries. *Electrochimica Acta* 215, 93–99. doi:10.1016/j.electacta.2016.08.081

Yue, J., Han, F., Fan, X., Zhu, X., Ma, Z., Yang, J., et al. (2017). High-Performance All-Inorganic Solid-State Sodium-Sulfur Battery. *ACS Nano* 11 (5), 4885–4891. doi:10.1021/acsnano.7b01445

Zhang, J., Zhong, H., Zheng, C., Xia, Y., Liang, C., Huang, H., et al. (2018a). All-solid-state Batteries with Slurry Coated LiNi0.8Co0.1Mn0.1O2 Composite Cathode and Li6PS5Cl Electrolyte: Effect of Binder Content. *J. Power Sourc.* 391, 73–79. doi:10.1016/j.jpowsour.2018.04.069

Zhang, Z., Shao, Y., Lotsch, B., Hu, Y.-S., Li, H., Janek, J., et al. (2018b). New Horizons for Inorganic Solid State Ion Conductors. *Energ. Environ. Sci.* 11 (8), 1945–1976. doi:10.1039/C8EE01053F

Zhou, W., Wang, S., Li, Y., Xin, S., Manthiram, A., and Goodenough, J. B. (2016). Plating a Dendrite-free Lithium Anode with a Polymer/ceramic/polymer sandwich Electrolyte. *J. Am. Chem. Soc.* 138 (30), 9385–9388. doi:10.1021/jacs.6b05341

Conflict of Interest: The authors declare that the research was conducted in the absence of any commercial or financial relationships that could be construed as a potential conflict of interest.

Publisher's Note: All claims expressed in this article are solely those of the authors and do not necessarily represent those of their affiliated organizations, or those of the publisher, the editors and the reviewers. Any product that may be evaluated in this article, or claim that may be made by its manufacturer, is not guaranteed or endorsed by the publisher.